CHAPTER 3

NEW TRINUCLEAR Ni^{II} COMPLEX CONTAINING INCOMPLETE CUBANE Ni_3O_4 CORE STRUCTURE

In the past decades, the design and investigation of polynuclear transition metal complexes have received an intense attention due to their potential application for single–molecule magnets (SMMs) [1–7]. One current research theme focuses on the synthesis of the cubane–like structures, *e.g.* Cu_4O_4 [1,5], Cd_4O_4 [2], Co_4O_4 [8–10] and Ni_4O_4 [3–6,11–13], and the containing incomplete cubane cores, *e.g.* Co_3O_4 [9, 14–17] and Fe_3O_4 [18], by using the multifunctional ligands such as chelating, bridging and terminal ligands simultaneously. The introduction of amino acid–containing ligands represents a promising route to the synthesis of the polynuclear clusters. These ligands have at least two parts that can bind to metal center including the N and O atoms of the NH_2 and the carboxylate groups. Additionally, they feature many biological applications such as antibacterial, antiviral and antifungal activities [19–23].

In this chapter, we report the preparation and crystal structure of divalent metal complexe, $[Ni_3(C_9H_{11}NO_3)_6(OCH_3)]\cdot4CH_3OH$ (**I**), which prepared and isolated from the reaction between nickel(II) nitrate hexahydrate, *S*–2–amino–2–methyl–3–(4'–hydroxyphenyl)propanoic acid or *L*–*p*–tyrosine (*L*–Tyr) and triethylamine as co−ligands in methanol solvent. Only the single crystal structure was however elucidated because there was not enough sample for the other characterization.

3.1 Experimental

3.1.1 Synthesis and crystal growth

$Ni(NO_3)_2{\cdot}6H_2O$ (0.0148 g, 0.5 mmol; Alfa Aesar, 98%) and 4−(HO)$C_6H_4CH_2CH(NH_2)CO_2H$ (*L*−Tyr; 0.0185 g, 0.10 mmol; Sigma−Aldrich, 98%) were dissolved in methanol (5.0 cm^3; Fisher Scientific, 99.8%) using a glass vial (vial **A**). A few drops of HCl (Fisher Scientific, 37%) were necessary to completely dissolve the *L*−Tyr. To a smaller glass vial, *ca*. 0.2 cm^3 of $(C_2H_5)_3N$ (triethylamine; Fisher Scientific, 99%) was added and the vial closed using lid with a small pin hole (vial **B**). Vial **B** was then inserted in vial **A**, which was then closed tightly. After *ca*. 4 months, a few blue block crystals crystallized from the solution, and were isolated for X−ray diffraction data collection. Due to a limited amount of the product, the other characterization could not be performed.

3.1.2 Single crystal structure determination

A full intensity data set of **I** was collected at 150(2) *K* using a Stöe IPDS2 image plate diffractometer operated with Mo *Kα* radiation, employing a single *ω*−scan. The structure was then solved by direct methods using SHELXS−97 *via* the WinGX program interface [24]. In order to take the contribution of disordered methanol solvent into account, the “SQUEEZE” option' in the program PLATON [25] was implemented after four molecules of CH_3OH were allocated in the structure. The reported number of 279 electrons to be found in the 1273 $Å^3$ or ~31% of the solvent accessible volume was determined. This value was expected for approximately 17 molecules of CH_3OH solvent. The application of SQUEEZE resulted in a significant improvement of the *R* and *Rw* values from 0.0734 and 0.2124 to 0.0401 and 0.0945, respectively. The crystallographic data, collection and refinement details are summarized in Table 3.1. The refined atomic coordinates and equivalent isotropic displacement parameters are provided in Table 3.2. The selected bond lengths and angles about the metal centers are listed in Table 3.3.

Table 3.1 Crystallographic data for structural solution and refinement of **I**.

Identification code	**I**
Empirical formula	$[Ni_3(C_9H_{11}NO_3)_6(OCH_3)]\cdot 4CH_3OH$
Formula weight	1400.28
Crystal system	Monoclinic
Space group	$P2_1/b$
Crystal size (mm^3)	0.36 × 0.35 × 0.34
a (Å)	12.5688(6)
b (Å)	25.3381(9)
c (Å)	13.1058(7)
β (°)	96.740(4)
V (Å^3)	4145.0(3)
Z	2
T (K)	150(2)
$\rho_{calc.}$ (g·cm^{-3})	1.122
μ (mm^{-1})	0.738
θ range (°)	1.61–26.14
λ (Mo Kα) (Å)	0.71073
R_{int}	0.074
Reflection collected	41350
Unique reflections	16565
Number of parameters	780
Number of restraints	1
R, Rw ($I > 2\sigma(I)$)	0.0401, 0.0945
R, Rw (all data)	0.0525, 0.0969
Goodness of fit	0.878

Table 3.2 Atomic coordinates and equivalent isotropic displacement parameters of non–hydrogen atoms for **I**.

	x	***y***	***z***	***Ueq*** **(Å^2)**
Ni1	0.67401(3)	0.209152(16)	0.66058(4)	0.03463(11)
Ni2	0.48220(3)	0.291099(15)	0.62530(4)	0.03586(11)
Ni3	0.64300(3)	0.280740(15)	0.46105(4)	0.03642(11)
O1	0.83540(19)	0.22349(9)	0.6684(2)	0.0369(6)
O2	0.9740(2)	0.25142(11)	0.7761(2)	0.0483(7)
O3	0.9161(3)	-0.01815(12)	0.6914(3)	0.0763(10)
O4	0.66026(18)	0.20168(9)	0.5025(2)	0.0370(6)
O5	0.7561(2)	0.16689(11)	0.3872(2)	0.0455(6)
O6	0.3242(2)	-0.01120(10)	0.4159(2)	0.0552(8)
O7	0.4971(2)	0.31369(9)	0.7749(2)	0.0407(6)
O8	0.5333(3)	0.38163(11)	0.8774(2)	0.0601(8)
O9	0.0065(2)	0.31212(11)	0.6231(2)	0.0548(7)
O10	0.50697(18)	0.21246(10)	0.6586(2)	0.0396(6)
O11	0.4391(2)	0.14462(10)	0.7387(2)	0.0448(6)
O12	0.0715(3)	0.10594(17)	0.3024(3)	0.0922(12)
O13	0.64711(19)	0.36165(10)	0.4467(2)	0.0436(7)
O14	0.7563(2)	0.42996(10)	0.4409(3)	0.0553(8)
O15	0.6373(3)	0.29244(14)	-0.0297(2)	0.0757(9)
O16	0.48472(19)	0.27843(10)	0.4722(2)	0.0409(6)
O17	0.3229(2)	0.26011(14)	0.3935(3)	0.0698(9)
O18	0.5789(2)	0.12088(11)	-0.1018(2)	0.0493(7)
O1M	0.64605(17)	0.28831(10)	0.62163(19)	0.0350(5)
O2M	0.8596(5)	0.1098(2)	0.2522(4)	0.1298(17)
O3M	1.0553(3)	-0.02010(15)	0.5593(3)	0.0815(10)
O4M	0.6264(6)	0.4805(3)	0.9009(6)	0.177(3)
O5M	0.3634(7)	0.3045(4)	1.0147(6)	0.215(3)
N1	0.7077(2)	0.21031(14)	0.8182(2)	0.0432(7)
N2	0.6949(2)	0.12825(11)	0.6396(3)	0.0416(8)
N3	0.4712(2)	0.37166(11)	0.6007(2)	0.0358(7)
N4	0.3258(2)	0.26513(11)	0.6264(3)	0.0389(7)
N5	0.8050(2)	0.28923(12)	0.4539(2)	0.0386(7)

Table 3.2 Atomic coordinates and equivalent isotropic displacement parameters of non–hydrogen atoms for **I** (continued).

	x	***y***	***z***	***Ueq*** **(Å^2)**
N6	0.5834(3)	0.26790(13)	0.3064(3)	0.0452(8)
C1	0.8803(3)	0.23246(14)	0.7588(3)	0.0404(9)
C2	0.8238(3)	0.21973(14)	0.8507(3)	0.0426(9)
C3	0.8785(3)	0.17307(16)	0.9118(3)	0.0477(10)
C4	0.8886(3)	0.12271(16)	0.8527(3)	0.0478(10)
C5	0.9647(3)	0.11715(17)	0.7819(4)	0.0558(11)
C6	0.9773(4)	0.07274(18)	0.7297(4)	0.0614(12)
C7	0.9103(4)	0.02862(17)	0.7426(4)	0.0590(12)
C8	0.8360(4)	0.03291(17)	0.8129(4)	0.0612(13)
C9	0.8280(3)	0.07957(17)	0.8676(4)	0.0567(11)
C10	0.7201(3)	0.16670(13)	0.4722(3)	0.0363(9)
C11	0.7544(3)	0.12247(13)	0.5498(3)	0.0405(9)
C12	0.7462(3)	0.06642(14)	0.5046(4)	0.0524(11)
C13	0.6346(3)	0.04650(13)	0.4814(3)	0.0420(9)
C14	0.5666(3)	0.06193(14)	0.3962(4)	0.0467(10)
C15	0.4626(3)	0.04394(14)	0.3745(4)	0.0473(10)
C16	0.4246(3)	0.00790(15)	0.4418(3)	0.0476(10)
C17	0.4897(3)	-0.00772(15)	0.5270(3)	0.0469(10)
C18	0.5934(3)	0.01222(16)	0.5464(3)	0.0501(10)
C19	0.5061(3)	0.36282(14)	0.7897(3)	0.0404(9)
C20	0.4830(3)	0.40097(13)	0.7005(3)	0.0368(8)
C21	0.3828(3)	0.43479(14)	0.7125(3)	0.0423(9)
C22	0.2789(3)	0.40506(13)	0.6917(3)	0.0390(9)
C23	0.2428(3)	0.37308(15)	0.7650(3)	0.0451(9)
C24	0.1507(3)	0.34206(15)	0.7456(3)	0.0434(9)
C25	0.0942(3)	0.34335(15)	0.6479(3)	0.0428(9)
C26	0.1283(3)	0.37557(17)	0.5735(4)	0.0528(11)
C27	0.2194(3)	0.40591(15)	0.5956(4)	0.0479(10)
C28	0.4328(3)	0.18951(14)	0.6989(3)	0.0360(8)
C29	0.3300(3)	0.22191(14)	0.7017(3)	0.0394(9)
C30	0.2260(3)	0.18813(15)	0.6932(3)	0.0425(9)

Table 3.2 Atomic coordinates and equivalent isotropic displacement parameters of non–hydrogen atoms for **I** (continued).

	x	***y***	***z***	***Ueq* (Å^2)**
C31	0.1882(3)	0.16788(15)	0.5888(3)	0.0462(10)
C32	0.0857(3)	0.18068(18)	0.5424(4)	0.0610(13)
C33	0.0455(4)	0.16009(19)	0.4494(4)	0.0635(13)
C34	0.1067(4)	0.1288(2)	0.3951(4)	0.0661(13)
C35	0.2115(4)	0.1169(2)	0.4365(5)	0.0740(16)
C36	0.2488(3)	0.13418(18)	0.5326(4)	0.0577(12)
C37	0.7391(3)	0.38049(14)	0.4409(3)	0.0422(9)
C38	0.8346(3)	0.34438(14)	0.4360(3)	0.0437(10)
C39	0.8885(3)	0.35072(18)	0.3408(4)	0.0565(11)
C40	0.8211(3)	0.33499(17)	0.2459(4)	0.0558(11)
C41	0.7431(4)	0.3691(2)	0.1951(4)	0.0692(14)
C42	0.6809(4)	0.3557(2)	0.1066(4)	0.0690(13)
C43	0.6922(3)	0.30699(17)	0.0614(3)	0.0530(11)
C44	0.7645(4)	0.27061(18)	0.1084(3)	0.0602(12)
C45	0.8300(3)	0.2852(2)	0.1989(3)	0.0555(10)
C46	0.4195(3)	0.26377(15)	0.3922(3)	0.0444(9)
C47	0.4695(3)	0.25007(15)	0.2987(3)	0.0442(9)
C48	0.4619(3)	0.18945(15)	0.2818(3)	0.0463(10)
C49	0.4916(3)	0.17103(14)	0.1804(3)	0.0416(9)
C50	0.4162(3)	0.17076(15)	0.0914(3)	0.0483(10)
C51	0.4432(3)	0.15440(15)	-0.0011(3)	0.0452(9)
C52	0.5463(3)	0.13756(15)	-0.0125(3)	0.0435(9)
C53	0.6209(3)	0.13709(17)	0.0737(3)	0.0522(11)
C54	0.5945(3)	0.15397(16)	0.1677(3)	0.0481(10)
C1M	0.7126(3)	0.32667(13)	0.6751(3)	0.0384(9)
C2M	0.8170(8)	0.0539(4)	0.2325(7)	0.140(3)
C3M	1.0306(5)	0.0038(3)	0.4648(5)	0.0954(18)
C4M	0.5490(9)	0.5181(5)	0.9249(9)	0.172(4)
C5M	0.2700(8)	0.3219(4)	1.0342(7)	0.142(3)

Table 3.3 Selected observed bond distances and angles in the compound **I**.

Bond distances (Å)			
Ni1–O1	2.051(2)	Ni2–O10	2.056(3)
Ni1–N1	2.060(3)	Ni2–N3	2.069(3)
Ni1–O4	2.067(3)	Ni2–N4	2.074(3)
Ni1–N2	2.089(3)	Ni3–O16	2.013(2)
Ni1–O1M	2.089(3)	Ni3–O13	2.060(3)
Ni1–O10	2.098(2)	Ni3–N5	2.060(3)
Ni2–O1M	2.067(2)	Ni3–N6	2.102(3)
Ni2–O7	2.030(3)	Ni3–O1M	2.109(2)
Ni2–O16	2.036(3)	Ni3–O4	2.080(2)
Bond angles (°)			
O1–Ni1–N1	82.06(11)	O10–Ni2–N3	174.38(12)
O1–Ni1–O4	91.83(10)	O1M–Ni2–N3	94.50(11)
N1–Ni1–O4	171.72(11)	O7–Ni2–N4	93.59(11)
O1–Ni1–N2	92.38(11)	O16–Ni2–N4	94.65(11)
N1–Ni1–N2	97.58(14)	O10–Ni2–N4	79.10(10)
O4–Ni1–N2	77.00(12)	O1M–Ni2–N4	159.52(10)
O1–Ni1–O1M	88.80(9)	N3–Ni2–N4	105.56(11)
N1–Ni1–O1M	103.90(12)	O16–Ni3–O13	94.09(10)
O4–Ni1–O1M	81.44(9)	O16–Ni3–N5	175.41(12)
N2–Ni1–O1M	158.43(11)	O13–Ni3–N5	81.74(11)
O1–Ni1–O10	167.32(10)	O16–Ni3–O4	91.53(10)
N1–Ni1–O10	95.69(11)	O13–Ni3–O4	168.31(11)
O4–Ni1–O10	91.47(10)	N5–Ni3–O4	92.24(11)
N2–Ni1–O10	100.29(11)	O16–Ni3–N6	79.74(12)
O1M–Ni1–O10	79.59(9)	O13–Ni3–N6	94.34(12)
O7–Ni2–O16	170.42(10)	N5–Ni3–N6	102.40(12)
O7–Ni2–O10	94.22(10)	O4–Ni3–N6	96.75(11)
O16–Ni2–O10	92.13(11)	O16–Ni3–O1M	80.37(9)
O7–Ni2–O1M	93.04(10)	O13–Ni3–O1M	90.18(11)
O16–Ni2–O1M	80.85(9)	N5–Ni3–O1M	97.66(10)
O10–Ni2–O1M	81.11(9)	O4–Ni3–O1M	80.65(10)
O7–Ni2–N3	82.47(11)	N6–Ni3–O1M	159.86(10)
O16–Ni2–N3	90.61(12)		

3.2 Results and discussion

A trinuclear nickel(II) complex of **I** was synthesized and characterized as a neutral charged cluster containing the incomplete cubane $\{Ni_3(\mu_3\text{–}O)(\mu_2\text{–}O)_2(\mu_1\text{–}O)\}$ core. The asymmetric unit contains a neutral cluster of ninety–one non–hydrogen atoms comprising three Ni ions, six tyrosinate ligands, a methoxy group and four methanol molecules, as shown in Fig. 3.1 with the atomic numbering scheme. The three Ni ions adopt similar octahedral coordination geometry, completed by two monodentate amino N atoms, one monodentate carboxylate O atom, two carboxylate bridging μ_2–O atoms, and one bridging μ_3–O atom of the methoxy group; $\{Ni(\mu_3\text{–}O)(\mu_2\text{–}O)_2(\mu_1\text{–}O)(\mu_1\text{–}N)_2\}$. The six tyrosinate ligands exhibit the common chelating mode of coordination, using the amino N atoms and either the carboxylate $\mu_2\text{–}\eta^2\text{:}\eta^0$ O atoms (O4, O10, O16) or the carboxylate $\mu_1\text{–}\eta^1\text{:}\eta^0$ O atoms (O1, O7, O13). These generate two five–membered chelate rings about each Ni center. These coordination modes are commonly found in the tyrosinate ligands [21–23]. Curiously, none of the phenolic groups of the tyrosine ligands within **I** are coordinated to the metal, despite conditions sufficiently basic to produce methoxide.

The three $\{Ni(\mu_3\text{–}O)(\mu_2\text{–}O)_2(\mu_1\text{–}O)(\mu_1\text{–}N)_2\}$ octahedra are condensed by edge–sharing and the addition of a $\mu_3\text{–}OCH_3$ group (O1M) results in a trinuclear cluster with the $\{Ni_3(\mu_3\text{–}O)(\mu_2\text{–}O)_2(\mu_1\text{–}O)\}$ incomplete cubane core (Fig. 3.2) [9, 18]. Notably, the nickel ions present within the cluster must display a total positive charge of +7 to balance the six tyrosinate ions and one methoxide ion. This corresponds to a mean oxidation state for the nickel of +2.33. Although the complete cubane core $[Ni_4O_4]$ is rather well illustrated within the CSD [26] with over 100 example, there are only 10 examples of the incomplete cubane core [Ni_3O_4] (see Refcodes ERUVIA and IHEKAI for examples), although the core within **I** is rather more symmetric than many of these examples.

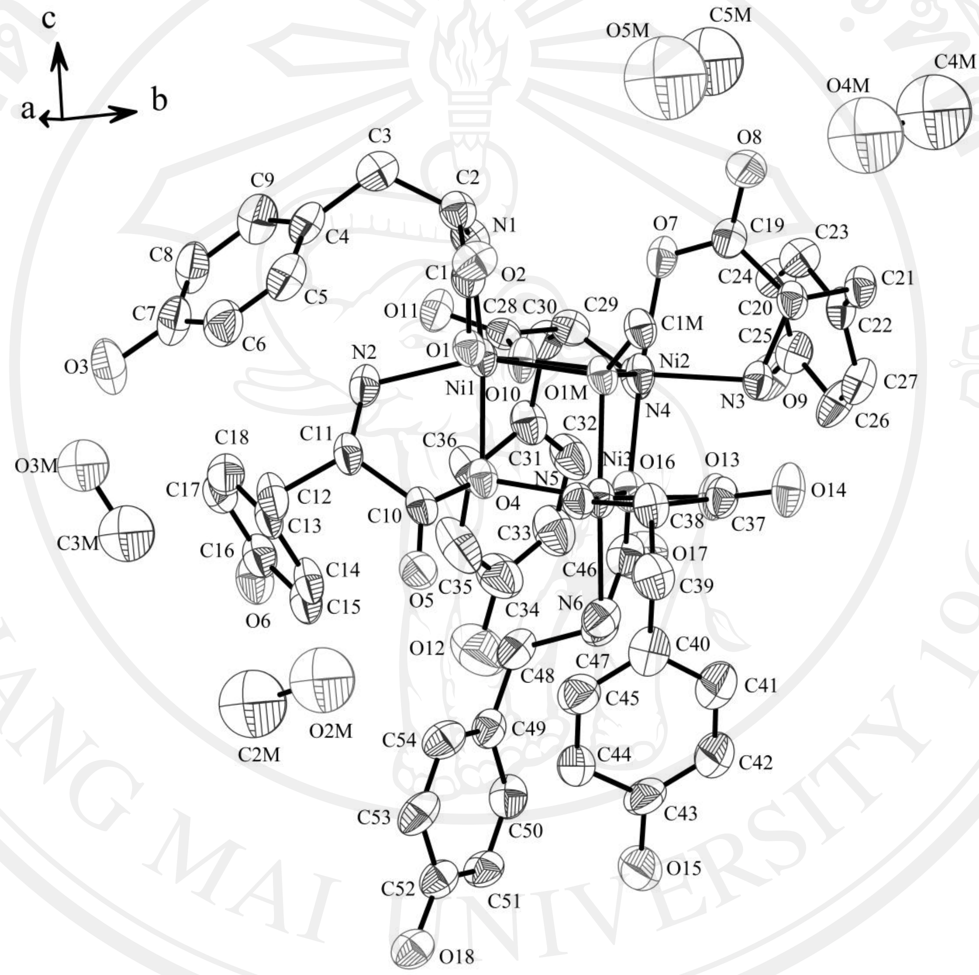

Fig. 3.1 The asymmetric unit of **I** showing atom−labeling scheme and with 50% probability displacement ellipsoids. Hydrogen atoms are omitted for clarity.

The summation of the inner angles for each quadrilateral face of the {$Ni_3(\mu_3{-}O)(\mu_2{-}O)_2(\mu_1{-}O)$} core, *i.e.* {Ni1–O10–Ni2–O1M}, {Ni1–O4–Ni3–O1M} and {Ni2–O16–Ni3–O1M}, of *ca.* 360° suggest the planarity of these faces.

Distributions of the Ni–μ_3–O1M distances and the Ni–μ_3–O1M–Ni angles in the ranges of 2.067(2)–2.109(2) Å and 97.17(10)–99.59(10)°, respectively, imply an asymmetrical arrangement of the three Ni ions about the apical μ_3–O1M atom. This is also evident from the distances between any two Ni ions which vary in a range of 3.132(1)–3.174(1) Å. These relatively short distances between pairs of Ni ions may signal the presence of weak metallic bonds within **I**. In nickel metal, the Ni–Ni distance is 2.49 Å, while within the CSD Ni^{II} to Ni^{II} distances lie in the range 2.194–3.441 Å [26]. The triangular arrangement of Ni ions within the cluster may also induce spin disorder and be associated with magnetic frustration [18, 27, 28].

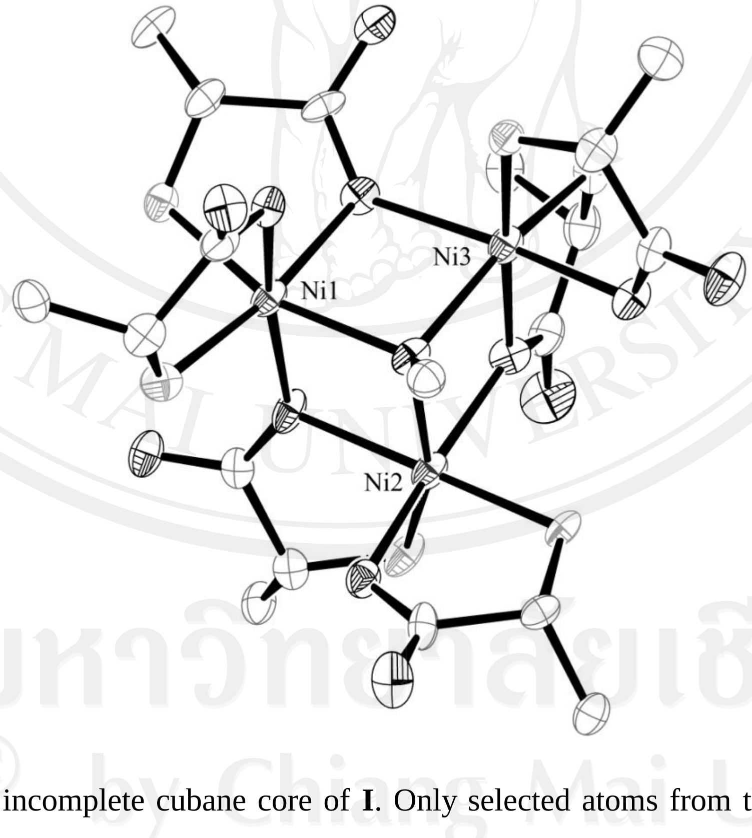

Fig. 3.2 The incomplete cubane core of **I**. Only selected atoms from the ligands are drawn. Atoms are shown as 30% probability ellipsoids.

According to previous literature [9], three inter–ligand (intra–cluster) hydrogen bonding interactions of N–H···O type were reported to be important in stabilizing the incomplete cubane structure. This seems to be partially true for the $\{Ni_3(\mu_3–O)(\mu_2–O)_2(\mu_1–O)\}$ core in **I**, in which three N–H···O hydrogen bonding interactions, *i.e.* N3–H3C···O13, N4–H4B···O17 and N5–H5A···O1 [N···O 3.050(5)–3.251(4) Å, N–H···O 142.00–149.89°], are present (Table 3.4 and Fig. 3.3a). Atoms N1 and N5, in addition, reinforce the stability of the $\{Ni_3(\mu_3–O)(\mu_2–O)_2(\mu_1–O)\}$ core *via* the inter–cluster interactions, *i.e.* N1–H1A···O15, N1–H1B···O18 and N5–H5A···O9 [N···O 3.042(4)–3.216(4) Å, N–H···O 132.69–156.47°] (Fig. 3.3b). The presence of the $–CH_2–$ group in the structure of the tyrosinate provides flexibility in spatial arrangement of the $–(C_6H_4)OH$ part, depending on surrounding environment. In the crystal structure of **I**, the arrangement of these motifs is regulated by the strong O–H···O hydrogen bonding interactions (Fig. 3.3b). The OH groups of all tyrosinate anions are associated in the O–H···O interactions with the neighboring clusters and methanol molecules [O–H···O 2.597(4)–2.983(4) Å, O–H···O 121.68–173.13°], and these generate the supramolecular assembly in **I**. The arrangement of these clusters occurs in such a way to maximize the hydrogen bonding interactions of which the weak hydrogen bonding of C–H···O type are also present, *i.e.* the intra–cluster C30–H30A···O11 and C54–H54···O5, and the inter–cluster C1M–H1M1···O1 and C38–H38···O9.

The clusters are arranged by the 2_1 screw axis into layers in the *xz* plane. These layers are stacked in an ABAB arrangement parallel to *b*–axis. There exist hydrogen bonds between the clusters, both within the layers and between them. This packing arrangement of clusters is rather inefficient and the structure contains large voids centered on the origin such that approximately 31% by volume of the structure is solvent accessible volume. Methanol molecules within these regions were poorly located and the reflection data were treated with the SQUEEZE algorithm [25] to model electron density within these regions. These calculations reveal that each void contains *ca.* 279 electrons consistent with around 17 molecules of methanol, giving an overall composition of $[Ni_3(C_9H_{11}NO_3)_6(OCH_3)]\cdot 21CH_3OH$ for **I**. The methanol evaporates very quickly when crystals are removed from solvent and this has prevented extensive analysis of the properties of **I**.

Table 3.4 Hydrogen bonding geometry for **I**.

D–H···A ^{a}	D–H, (Å)	H···A, (Å)	D···A, (Å)	∠ D–H···A, (°)
O3–H3··· O3M	0.8200	1.7897	2.602(5)	170.20
O6–H6A··· O14^{iii}	0.8200	1.8818	2.685(4)	166.18
O9–H9A··· O2^{iv}	0.8200	1.7809	2.597(4)	173.13
O12–H12··· O2M^{iv}	0.8200	1.9026	2.669(7)	155.15
O15–H15A··· O7^{v}	0.8200	2.4692	2.983(4)	121.68
O15–H15A··· O8^{v}	0.8200	2.0183	2.815(4)	163.92
O18–H18A··· O11^{v}	0.8200	1.8438	2.638(4)	162.55
N1–H1A··· O15^{i}	0.9000	2.2594	3.082(4)	151.85
N1–H1B··· O18^{i}	0.9000	2.1954	3.042(4)	156.47
N3–H3C··· O13	0.9000	2.3633	3.174(4)	149.89
N4–H4B··· O17	0.9000	2.2903	3.050(5)	142.00
N5–H5A···O1	0.9000	2.4645	3.251(4)	146.11
N5–H5A··· O9^{ii}	0.9000	2.5373	3.216(4)	132.69
C1M–H1M1···O1	0.9600	2.5211	3.042(4)	114.10
C30–H30A···O11	0.9700	2.5512	2.893(5)	100.72
C38–H38··· O9^{ii}	0.9800	2.3784	3.178(5)	138.39
C54–H54···O5	0.9300	2.4245	3.338(5)	167.25

^{a}Symmetry codes: (i) *x*, *y*, 1 + *z*; (ii) 1 + *x*, *y*, *z*; (iii) 1 - *x*, -1/2 + *y*, 1 - *z*; (iv) -1 + *x*, *y*, *z*; (v) *x*, *y*, -1 + *z*

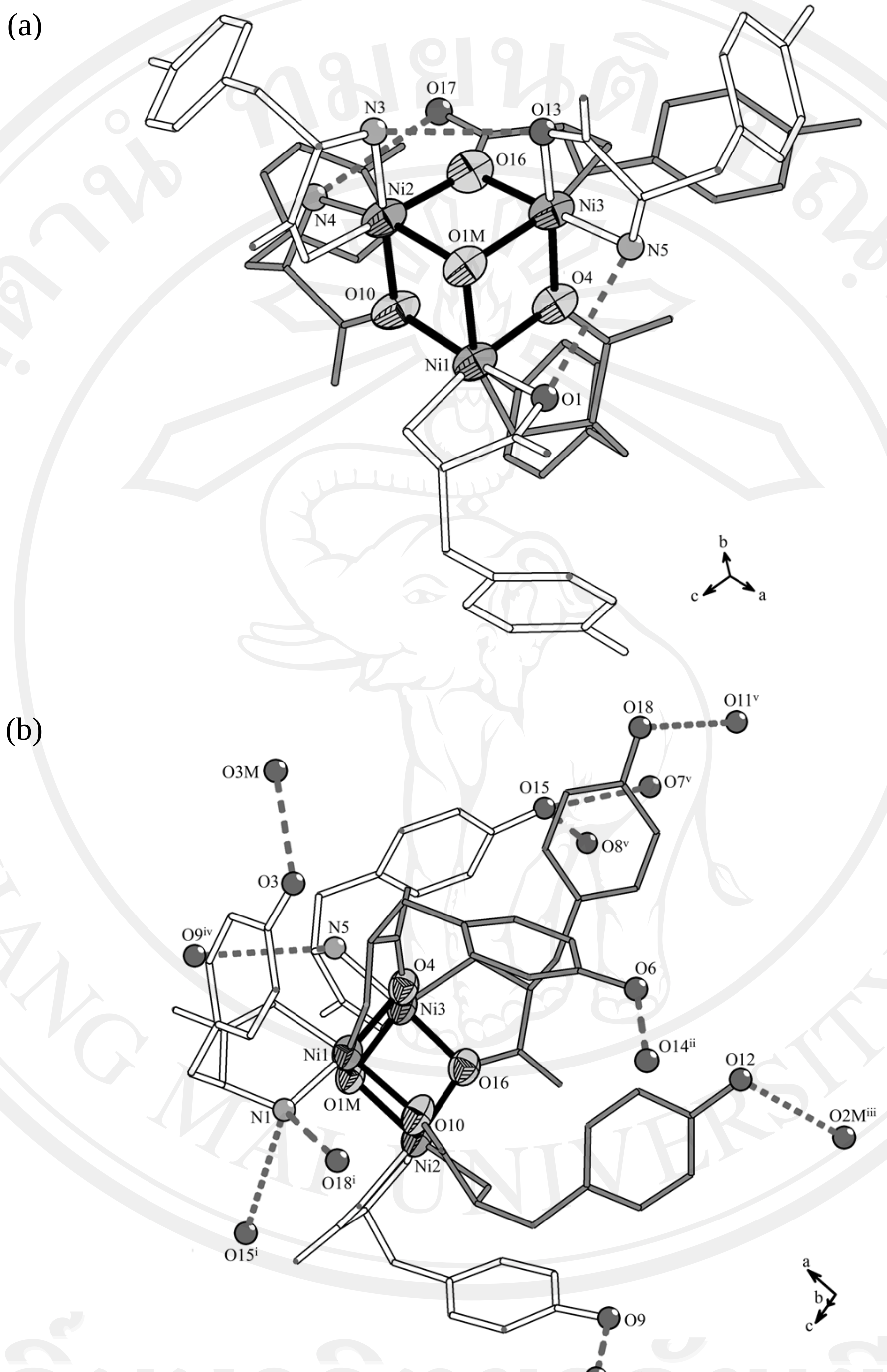

Fig. 3.3 View of (a) intra−cluster and (b) inter−cluster hydrogen bonding interactions (dash lines), showing the donor and acceptor atoms by ball−and−stick model and with 50% probability displacement ellipsoids for the incomplete cubane core. Weak C−H···O hydrogen bonding interactions are omitted.

The presence of methoxide suggests that it should be possible to obtain similar structures with other weakly coordinating anions. Similarly, replacement of methamol by other bulkier and less volatile solvents, may enable further studies on similar compounds, in particular magnetic measurements. Clusters of this type therefore may be suitable for fundamental magnetic studies by variation of ligand bulk, or may prove suitable nodes in the construction of framework solids by appropriate ligand choice.

3.3 Conclusions

A trinuclear nickel complex $[Ni_3(C_9H_{11}NO_3)_6(OCH_3)]\cdot 4CH_3OH$ was synthesized and characterized as a neutral cluster containing the incomplete cubane $\{Ni_3(\mu_3{-}O)(\mu_2{-}O)_2(\mu_1{-}O)\}$ core. The three Ni ions show similar octahedral coordination, $\{Ni(\mu_3{-}O)(\mu_2{-}O)_2(\mu_1{-}O)(\mu_1{-}N)_2\}$. The common coordination modes, *i.e.* chelating (*via* the amino N and the carboxylate O atoms) and bridging (*via* the carboxylate O atom), are exhibited by the tyrosinates. Three inter–ligand (intra–cluster) N–H···O hydrogen bonding interactions stabilize the incomplete cubane structure. Additional N–H···O, O–H···O and C–H···O interactions formed between the clusters and methanol molecules regulate the spatial orientation of the tyrosinate and the assembly of the clusters in the crystal. The structure contains approximately 31% solvent accessible volume between the clusters. This is filled with disordered methanol. The approximate equilateral triangular arrangement of the three Ni ions in the incomplete cubane structure suggests the possible magnetic frustration, and the proximity of these metal centers indicates weak metallic bonds.

REFERENCES

1. J. Chakraborty, S. Thakurta, G. Pilet, D. Luneau, S. Mitra, Polyhedron 28 (2009) 819.
2. M.–C. Suen, J.–C. Wang, Inorg. Chem. Commun. 9 (2006) 478.
3. S.H. Zhang, Y.D. Zhang, H.H. Zou, J.J. Guo, H.P. Li, Y. Song, H. Liang, Inorg. Chim. Acta. 396 (2013) 119.
4. S.–Y. Zhang, W.–Q. Chen, B. Hu, Y.–M. Chen, W. Li, Y. Li, Inorg. Chem. Commun. 16 (2012) 74.
5. Y.–M. Li, J.–J. Zhang, R–B. Fu, S. –C. Xiang, T.–L. Sheng, D.–Q. Yuan, X.–H. Huang, X.–T. Wu, Polyhedron 25 (2006) 1618.
6. Y. Xiao, S.H. Zhang, G. Z. Li, Y.G. Wang, C. Feng, Inorg. Chim. Acta. 366 (2011) 39.
7. X. Song, Y. Xu, L. Li, D. Liao, Z. Jiang, Inorg. Chim. Acta. 360 (2007) 2039.
8. X. Zhang, W. You, Z. Zhu, L. Dang, Z. Sun, X. Zheng, Inorg. Chem. Commun. 9 (2006) 526.
9. T. Ama, Md.M. Rashid, T. Yonemura, H. Kawaguchi, T. Yasui, Coord. Chem. Rev. 198 (2000) 101.
10. K.E. Gubina, V.A. Ovchynnikov, J. Swiatek−Kozlowska, V.M. Amirkhanov, T.Y. Sliva, K.V. Domasevitch, Polyhedron 21 (2002) 963.
11. Q. Liang, R. Huang, X. Chen, Z. Li, X. Zhang, B. Sun, Inorg. Chem. Commun. 13 (2010) 1134.
12. X. Song, Y. Xu, L. Li, D. Liao, Z. Jiang, Inorg. Chim. Acta. 360 (2007) 2039.

13. A. Escuer, M. Font−Bardía, S.B. Kumar, X. Solans, R. Vicente, Polyhedron 18 (1999) 909.
14. T. Ama, T. Yonemura, S. Morita, M. Yamaguchi, Acta. Cryst. E66 (2010) m483.
15. T. Ama, M. Shiro, A. Takeuchi, T. Yonemura, H.Kawaguchi, T. Yasui, Bull. Chem. Soc. Jpn. 70 (1997) 2685.
16. T. Ama, Md.M. Rashid, A.K. Sarker, H. Miyakawa, T. Yonemura, H. Kawaguchi, T. Yasui, Bull. Chem. Soc. Jpn. 74 (2001) 2327.
17. T. Ama, T. Yonemura, M. Yamaguchi, Bull. Chem. Soc. Jpn. 79 (2006) 1063.
18. M. Lalia−Kantouri, C.D. Papadopoulos, A.G. Hatzidimitriou, T. Bakas, S. Pachini, Z. Anorg. Allg. Chem. 636 (2010) 531.
19. J. Weng, M. Hong, Q. Shi, R. Cao, A.S.C. Chan, Eur. J. Inorg. Chem. (2002) 2553.
20. T. Sugimori, H. Masuda, N. Ohata, K. Koiwai, A. Odani, O. Yamauchi, Inorg. Chem. 36 (1997) 576.
21. Y. Pei, L. Wang, Acta Cryst. E62 (2006) m1668.
22. A. Wojciechowska, M. Daszkiewicz, Z. Staszak, A. Trusz−Zdybek, A. Bieńko, A. Ozarowskiz, Inorg. Chem. 50 (2011) 11532.
23. A. Wojciechowska, A. Gagor, R. Wysokinski, A. Trusz−Zdybek, J. Inorg. Biochem. 117 (2012) 93.
24. G.M. Sheldrick, Acta Cryst. A64 (2008) 112.
25. A. L. Spek, J. Appl. Cryst. 36 (2003) 7.
26. F.R. Allen, Acta Cryst. B58 (2002) 380.

27. D.N. Hendrickson, E.–C. Yang, R.M. Isidro, C. Kirman, J. Lawrence, R.S. Edwards, S. Hill, A. Yamaguchi, H. Ishimoto, W. Wernsdorfer, C. Ramsey, N. Dalal, M.M. Olmstead, Polyhedron 24 (2005) 2280.

28. S. Nakatsuji, Y. Nambu, H. Tonomura, O. Sakai, S. Jonas, C. Broholm, H. Tsunetsugu, Y. Qiu, Y. Maeno, Science 309 (2005) 1607.